Published in final edited form as:
Nature. 2013 November 21; 503(7476): 392–396. doi:10.1038/nature12631.

A canonical to non-canonical Wnt signalling switch in haematopoietic stem-cell ageing

Maria Carolina Florian[1], **Kalpana J. Nattamai**[2], **Karin Dörr**[1], **Gina Marka**[1], **Bettina Überle**[1], **Virag Vas**[1], **Christina Eckl**[3], **Immanuel Andrä**[4], **Matthias Schiemann**[4], **Robert A. J. Oostendorp**[3], **Karin Scharffetter-Kochanek**[1], **Hans Armin Kestler**[5], **Yi Zheng**[2], and **Hartmut Geiger**[1,2]

[1]Department of Dermatology and Allergic Diseases, University of Ulm, 89091 Ulm, Germany

[2]Division of Experimental Hematology and Cancer Biology, Cincinnati Children's Hospital Medical Center and University of Cincinnati, Cincinnati, Ohio 45229, USA

[3]3rd Department of Internal Medicine, Klinikum rechts der Isar, Technische Universität München, 81675 München, Germany

[4]Institute of Medical Microbiology, Immunology and Hygiene, Technische Universität München, 81675 München, Germany

[5]Institut für Neuroinformatik, Department of Bioinformatics and Systems Biology, University of Ulm, 89091 Ulm, Germany

Abstract

Many organs with a high cell turnover (for example, skin, intestine and blood) are composed of short-lived cells that require continuous replenishment by somatic stem cells[1,2]. Ageing results in the inability of these tissuesto maintain homeostasis and it is believed that somatic stem-cell ageing is one underlying cause of tissue attrition with age or age-related diseases. Ageing of haematopoietic stem cells (HSCs) is associated with impaired haematopoiesis in the elderly[3–6]. Despite a large amount of data describing the decline of HSC function on ageing, the molecular mechanisms of this process remain largely unknown, which precludes rational approaches to attenuate stem-cell ageing. Here we report an unexpected shift from canonical to non-canonical Wnt signalling in mice due to elevated expression of Wnt5a in aged HSCs, which causes stem-cell ageing. Wnt5a treatment of young HSCs induces ageing-associated stem-cell apolarity, reduction of regenerative capacity and an ageing-like myeloid–lymphoid differentiation skewing via

Correspondence and requests for materials should be addressed to H.G. (hartmut.geiger@uni-ulm.de)..

Author Contributions M.C.F. andH.G. designed and interpreted experiments and wrote the manuscript. M.C.F., K.J.N., B.Ü., C.E., M.S. I.A. and R.A.J.O. performed and analysed experiments. H.G. helped to perform transplantation experiments. V.V. helped with the Wnt5a mouse colony and performed inverse transplantation experiments and prepared sorted stroma CD45^{-} cells. K.D. and G.M. assisted in transplantation procedures and supported in cell sorting and flow analysis procedures. H.A.K. performed expression and databaseanalyses. Y.Z. and K.S.-K. assisted indesigning and interpreting experiments.

The authors declare no competing financial interests.

Online Content Any additional Methods, Extended Data display items and Source Data are available in the online version of the paper; references unique to these sections appear only in the online paper.

Supplementary Information is available in the online version of the paper.

activation of the small Rho GTPase Cdc42. Conversely, Wnt5a haploinsufficiency attenuates HSC ageing, whereas stem-cell-intrinsic reduction of Wnt5a expression results in functionally rejuvenated aged HSCs. Our data demonstrate a critical role for stem-cell-intrinsicnon-canonical Wnt5a signalling in HSC ageing.

Aged muscle stem cells can regenerate muscles as efficiently as young muscle stem cells either by forced activation of Notch, or by parabiosis-mediated inhibition of Wnt signalling[7–10]. Whether there is a similar critical role of Wnt signalling in ageing of HSCs remains largely unexplored. Multiple members of the Wnt family are expressed in haematopoietic cells as well as in non-haematopoietic stroma cells (for a concise review see ref. 11). Wnt3a (associated with canonical Wnt signalling) and Wnt5a (associated with non-canonical signalling) are so far the most studied Wnt proteins in haematopoiesis[12–16].

Notably, high levels of *Wnt5a* as well as *Wnt4* mRNA were detected in middle-aged (10 months) and aged (20–24 months old) long-term (LT)-HSCs (Lin^-, $Sca\text{-}1^+$, $c\text{-}Kit^+$, $CD34^-$, $Flk2^-$) and Lin^- cells from C57BL/6 as well as DBA/2 mice, whereas they were almost absent in young (2–3 months old) cells (Fig. 1a and Extended Data Fig. 1a–c), concurrently with elevated Wnt5a protein levelsin aged haematopoietic cells (Fig. 1b, c). Other Wnt proteins (including canonical-signalling-associated Wnt1, Wnt3a, Wnt5b and Wnt10b) did not present with changes in expression on ageing. In young LT-HSCs, Wnt5a localizes mainly at the plasma membrane, whereas aged LT-HSCs showed Wnt5a distributed primarily within the cytoplasm (Extended Data Fig. 1d–g and Supplementary Video 1). Wnt5a localization only partially overlapped with clathrin-positive vesicular structures in aged LT-HSCs (Extended Data Fig. 1f).

In young LT-HSCs,β-catenin islocalized mainly in the nucleus, indicative of active canonical Wnt signalling (Fig. 1d, e and Supplementary Video 2). Wnt5a has been reported to directly inhibit canonical Wnt signalling in haematopoietic cells[12]. Consistent with this finding, aged LT-HSCs presented with a reduced level and primarily cytoplasmiclocalization of β-catenin (Fig. 1d, e and Supplementary Video 3). Reduced levels of β-catenin upon ageing were specific to the LT-HSC compartment, as more differentiated LKs ($Lin^-c\text{-}Kit^+Sca\text{-}1^-$ cells), LSKs ($Lin^-Sca\text{-}1^+c\text{-}Kit^+$ cells), lymphoid-primed multipotent progenitors (LMPPs; $Lin^-c\text{-}Kit^+Sca\text{-}1^-CD34^+Flk2^+$ cells) and short-term (ST)-HSCs ($Lin^-c\text{-}Kit^+Sca\text{-}1^-CD34^+Flk2^-$ cells) (Extended Data Fig. 1h) showed similar levels of β-catenin upon ageing (Fig. 1g and Extended Data Fig. 1i). Axin2 (an established direct downstream target of canonical Wnt signalling[9,15]) transcript levels in aged LT-HSCs were markedly decreased (Fig. 1f). Young LT-HSCs treated with Wnt5a elicited a reduction in the level of β-catenin similar to the level found in aged LT-HSCs (Fig. 1g and Extended Data Fig. 1i). The presence of MG-132 (a proteasomal inhibitor) abolishes the reduction of β-catenin, whereas β-catenin degradation is already visible 2 h after Wnt5a exposure (Fig. 1h, i), indicating a direct action of Wnt5a on β-catenin levels. Our data support that on ageing, LT-HSCs shift from canonical to non-canonical Wnt signalling due to, at least in part, elevated Wnt5a expression and signalling in aged LT-HSCs.

In young HSCs a Wnt5a-driven non-canonical signalling pathway regulates quiescence via regulating the activity of the small Rho GTPase Cdc42 (refs 17–19). We recently

demonstrated a critical role for elevated Cdc42 activity in ageing and polarityofLT-HSCs[20].Bone-marrow-derived haematopoietic progenitor/stem cells treated *in vitro* with Wnt5a showed increased Cdc42 activity (Cdc42–GTP) (Fig. 2a, b). Elevated Cdc42 activity in aged HSCs is associated with a high percentage of LT-HSCs being apolar for tubulin and Cdc42, and this apolarity is a hallmark of aged LT-HSCs[20,21]. We detected an increased frequency of apolar cells among young Wnt5a-treated LT-HSCs (Fig. 2c, d and Extended Data Fig. 2a) to a level previously described for aged LT-HSCs. When Wnt5a was administered together with casin (a selective inhibitor of Cdc42 activity[20,22]), the frequency of polarized LT-HSCs did not change (Fig. 2c, d and Extended Data Fig. 2a), supporting the hypothesis that Wnt5a results in apolarity through increasing Cdc42 activity. Notably, Wnt5a treatment also induced apolarity for NCam2,an adhesion receptor molecule located on the cell membrane (Extended Data Fig. 2b, c). Wnt5a treatment did not alter mRNA expression of *Cdc42* (Extended Data Fig. 2d). *Rac2* and the Cdc42-related genes *Rhoj* and *Rhoq* showed slightly higher expression in aged compared to young LT-HSCs. Our data support the hypothesis that Wnt5a has a direct effect on Cdc42 activity and polarity establishment, as these changes were induced 2 h after Wnt5a treatment (Fig. 2a, b), although they do not exclude additional indirect effects (see also Extended Data Fig. 5).

Competitive transplant experiments (Extended Data Fig. 2e) revealed that *ex vivo* Wnt5a-treated young LT-HSCs presented with reduced engraftment and an ageing-like skewing in differentiation potential (elevated donor-derived myeloid contribution, reduced donor-derived B-cell contribution; Fig. 2e, f). When Wnt5a treatment was performed in the presence of casin, this ageing-associated differentiation skewing was not observed (Fig. 2f), confirming again the role of a Wnt5a–Cdc42 signalling axis in inducing ageing-like phenotypes in LT-HSCs. Treatment of young LT-HSCs with casin alone had no effect on engraftment potential and differentiation of HSCs, in agreement with previous data[20].

We next investigated haematopoiesis in mice haploinsufficient for Wnt5a ($Wnt5a^{+/-}$ mice; $Wnt5a^{-/-}$ mice are embryonic lethal[23]). Expression of Wnt5a and the activity of Cdc42 were increased on ageing in wild-type cells (Fig. 3a–d), whereas levels in aged $Wnt5a^{+/-}$ haematopoietic cells were similar to those in $Wnt5a^{+/-}$ and $Wnt5a^{+/+}$ young cells (Fig. 3a–d). Aged $Wnt5a^{+/-}$ LT-HSCs presented with a frequency of polarized cells similar to that found in young $Wnt5a^{+/-}$ and $Wnt5a^{+/+}$ LT-HSCs (Fig. 3e and Extended Data Fig. 3l, m). The frequency of B cells in aged $Wnt5a^{+/-}$ mice compared to aged wild-type mice was significantly increased, paralleled by a decreased myeloid cell frequency (Fig. 3f). Furthermore, total white blood cell, lymphocyte and red blood cell parameters of aged haploinsufficient $Wnt5a^{+/-}$ mice were similar to that of young wild-type and young $Wnt5a^{+/-}$ mice (Extended Data Fig. 3a–d). Moreover, whereas aged $Wnt5a^{+/+}$ mice, as expected, showed an increase in the frequency of both LSKs (Extended Data Fig. 3e) and LT-HSCs (Fig. 3g), aged haploinsufficient $Wnt5a^{+/-}$ mice exhibited a reduced frequency of both LSKs and LT-HSCs compared to control aged mice (Fig. 3g and Extended Data Fig. 3e). Notably, expression levels of Wnt5a in LT-HSCs, although elevated compared to young LT-HSCs, were almost an order of magnitude lower compared to the level of expression in $CD45^{-}$ stroma cells (Extended Data Fig. 3f). On ageing, levels of *Wnt5a* mRNA in stroma were reduced (Extended Data Fig. 3f). Experiments in which wild-type cells were

transplanted into *Wnt5a*$^{+/-}$ and *Wnt5a*$^{+/+}$ recipients revealed that the attenuation of ageing in haematopoiesis in aged *Wnt5a*$^{+/-}$ mice was due to changes in *Wnt5a* levels in haematopoietic cells (Extended Data Fig. 3g–k).

Finally, we asked whether inhibition of LT-HSC cell-intrinsic Wnt5a expression through a lentiviral short hairpin RNA (shRNA) approach might functionally rejuvenateaged LT-HSCs in transplantation settings (Fig. 4a and Extended Data Fig. 4a–c). Mice transplanted with aged, untransduced Ly5.2^{+} cells as well as with aged scrambled non-targeting shRNA (NT-GFP^{+}Ly5.2^{+}) cells showed an elevated frequency of myeloid cells but compromised lymphopoiesis (either B or T cells or both) in both peripheral blood and bone marrow 24 weeks after transplant (Fig. 4b and Extended Data Fig. 4d), and thus the expected aged haematopoietic profile. In contrast, haematopoiesis in mice transplanted with a shRNA specific for *Wnt5a* (Wnt5a^{KD}-GFP^{+}Ly5.2) presented with improved B lymphopoiesis and a reduction in myeloid skewing, showing a bone marrow and peripheral blood differentiation profile overall more similar to the one characteristic of young mice (Fig. 4b and Extended Data Fig. 4d). In accordance with stem-cell rejuvenation, thefrequencyofdonor-derivedLT-HSCswasreducedinmicetransplanted with aged Wnt5a knockdown (Wnt5a^{KD}) cells compared to mice transplanted with aged non-targeting shRNA or untransduced cells (Fig. 4c). This Wnt5a knockdown effect was specific to aged cells because young Wnt5a knockdown cells performed very similar to controls (Extended Data Fig. 4e–g). In addition, the activity of Cdc42 was reduced in donor-derived Wnt5a knockdown cells whereas total Cdc42 protein levels were unchanged (Fig. 4d, e and Extended Data Fig. 4h), and Wnt5a^{KD} LT-HSCs from recipient mice presented with a significantly elevated frequency of polarized cells compared to controls (Fig. 4f and Extended Data Fig. 4i, j). Moreover, aged Wnt5a^{KD} LT-HSCs reverted to a high expression level and nuclear localization of β-catenin, and therefore to active canonical Wnt signalling (Fig. 4g, h and Extended DataFig.4k).In summary, reduction of ageing-associated elevated Wnt5a expression rejuvenates chronologically aged LT-HSCs.

Cross-talk between Wnt and Notch pathways, as reported for muscle stem cells, has not yet been investigated in HSC ageing. Aged LT-HSCs presented with a distinct pattern of expression activation of Notch ligands, receptors and Hes1 (a direct target indicative of active Notch pathway) (Extended Data Fig. 5a–g). This ageing-related Notch pathway activation was to a great extent recapitulated in young *Wnt5a*-treated LT-HSCs (Extended Data Fig. 5a–g). The non-canonical *Wnt5a* signalling pathway can also trigger Ca^{2+} influx in the cytoplasm and activate CamKII (calmodulin-dependent protein kinase II) and the calcium-sensitive transcription factor NFATc[3,24]. LT-HSCs presented with a biphasic (a short-term steep increase, followed by a lower, but long-term sustained signal) influx of Ca^{2+} in the cytoplasm in response to Wnt5a treatment (Extended Data Fig. 5l) and an increase in the level of p-CamKII (the phosphorylated active fraction of CamKII; total CamKII levels were unaltered or even decreased) and in the level of NFATc as determined by immunofluorescence staining (Extended Data Fig. 5h–k). Furthermore, the levels of both *p57* and *p27* mRNAs (which have been associated with stem-cell quiescence) were increased in aged and in young Wnt5a-treated LT-HSCs compared to young cells (Extended Data Fig. 5m), whereas cell-cycle parameters of LT-HSCs do not change with age[20]. These

data indicate that there might be crosstalk between the intrinsically increased Wnt5a/Cdc42 non-canonical Wnt pathway and the Notch1 pathway, eliciting Ca^{2+} signalling that ultimately increases quiescence[25] and self-renewal of LT-HSCs, which over time translates into an increased number of stem cells with a reduced engraftment potential. Further investigations are warranted to test this hypothesis in more detail (Extended Data Fig. 6).

We present here a novel concept that ageing of LT-HSCs is driven by a shift from canonical Wnt to non-canonical Wnt–Cdc42 signalling. The initiating event is interestingly stem-cell intrinsic (increase of Wnt5a expression in LT-HSCs on ageing). The mechanisms inducing elevated Wnt5a expression in aged LT-HSCs are currently unknown, but possibly involve epigenetic mechanisms[26]. Our data do not exclude action of stroma-derived Wnt proteins on more differentiated primitive haematopoietic cells or on LT-HSCs in distinct niches[20,27] or under situations of stress. Whereas we demonstrate a causative role for Wnt5a-induced Cdc42 signalling in HSC ageing, Wnt5a-induced non-canonical signalling could elicit additional changes that might, in addition to Cdc42, contribute to the ageing phenotype.

METHODS SUMMARY

C57BL/6 mice (10–12-week-old) were obtained from Janvier. Aged C57BL/6 mice (20–26-month-old) were obtained from the internal divisional stock (derived from mice obtained from both The Jackson Laboratory and Janvier) as well as from NIA/ Charles River. Samples were imaged with an AxioObserver Z1 microscope (Zeiss) or with an LSM710 confocal microscope (Zeiss). Primary raw data were imported into the Volocity Software package (Version 6.0, Perkin Elmer) for further processing and conversion into three-dimensional images. For reverse transcriptase real time PCR 20,000–40,000 LT-HSCs from young and aged mice were lysed and processed for RNA extraction immediately after sorting. RNA was obtained with the microRNA extraction kit (Qiagen) and all was used for cDNA conversion. cDNA was prepared and amplified with Ovation RNA Amplification system V2 (NuGEN). Relative levels of GTP-bound Cdc42 were determined by an effector pull-down assay. The lentivirus plasmid vector pLKO.1-YFP and KD sequences were obtained from Sigma's validated genome-wide TRC shRNA libraries.

METHODS

Mice

C57BL/6 mice (10–12-week-old) were obtained from Janvier. Aged C57BL/6 mice (20–26-month-old) were obtained from the internal divisional stock (derived from mice obtained from both The Jackson Laboratory and Janvier) as well as from NIA/Charles River. Congenic C57BL/6.SJL-*Ptprc*^{a}/Boy (BoyJ) mice were obtained from Charles River Laboratories or from the internal divisional stock (derived from mice obtained from Charles River Laboratories). Wnt5a mice were obtained from T. Yamaguchi. All mice were housed in the animal barrier facility under pathogen-free conditions either at the University of Ulm or at CCHMC. All mouse experiments were performed in compliance with the German Law for Welfare of Laboratory Animals and were approved by the Institutional Review Board of the University of Ulm or by the IACUC of CCHMC.

LT-HSC competitive transplantation

For competitive LT-HSC transplantation, young (2–4-month-old) C57BL/6 mice (Ly5.2$^+$) were used as donors. Two-hundred LT-HSCs were sorted into 96 multi-well plates and cultured for 16 h in HBSS 1 10% FBS with or without 100 ng ml^{-1} Wnt5a (R&D System) in a water-jacketed incubator at 37 °C, 5% CO_2, 3% O_2. Stem cells were then mixed with 3 × 10^5 bone marrow cells from young (2–4-month-old) BoyJ competitor mice (Ly5.1$^+$) and transplanted into BoyJ recipient mice (Ly5.1$^+$). Peripheral blood chimaerism was determined by FACS analysis every 8 weeks up to 24 weeks after primary transplants. The transplantation experiment was performed four times with a cohort of five recipient mice per group each transplant. Inverse transplantation experiments were performed by lethally irradiating recipient *Wnt5a*$^{+/+}$ and *Wnt5a*$^{+/-}$ mice (Ly5.2$^+$). 2 × 10^6 total bone marrow cells from donor BoyJ mice (Ly5.1$^+$) were injected into each recipient mouse and transplanted mice were followed and bled every month for up to 20 months after transplantation. In general, transplanted mice were regarded as engrafted when peripheral blood chimaerism was higher or equal to 1.0% and contribution was detected in all lineages.

Flow cytometry and cell sorting

PB and bone marrow cell immunostaining was performed according to standard procedures and samples were analysed on a LSRII flow cytometer (BD Biosciences). Monoclonal antibodies to Ly5.2 (clone 104, eBioscience) and Ly5.1 (clone A20, eBioscience) were used to distinguish donor from recipient and competitor cells. For peripheral blood and bone marrow lineage analysis the antibodies used were all from eBioscience: anti-CD3ε (clone 145-2C11), anti-B220 (clone RA3-6B2), anti-Mac-1 (clone M1/70) and anti-Gr-1 (clone RC57BL/6-8C5). Lineage FACS analysis data are plotted as the percentage of B220$^+$, CD3$^+$ and myeloid (Gr-1$^+$, Mac-1$^+$ and Gr-1$^+$Mac-1$^+$) cells among donor-derived Ly5.2$^+$ cells in case of a transplantation experiment or among total white blood cells. As for early haematopoiesis analysis, mononuclear cells were isolated by low-density centrifugation (Histopaque 1083, Sigma) and stained with a cocktail of biotinylated lineage antibodies. Biotinylated antibodies used for lineage staining were all rat anti-mouse antibodies: anti-CD11b (clone M1/70), anti-B220 (clone RA3-6B2), anti-CD5 (clone 53-7.3) anti-Gr-1 (clone RB6-8C5), anti-Ter119 and anti-CD8a (clone 53-6.7) (all from eBioscience). After lineage depletion by magnetic separation (Dynalbeads, Invitrogen), cells were stained with anti-Sca-1 (clone D7) (eBioscience), anti-c-Kit (clone 2B8) (eBioscience), anti-CD34 (clone RAM34) (eBioscience), anti-CD127 (clone A7R34) (eBioscience), anti-Flk-2 (clone A2F10) (eBioscience) and streptavidin (eBioscience). Early haematopoiesis FACS analysis data were plotted as percentage of long-term haematopoietic stem cells (LT-HSCs, gated as LSK CD34$^{-/low}$Flk2$^-$), short-term haematopoietic stem cells (ST-HSCs, gated as LSK CD34$^+$Flk2$^-$) and lymphoid-primed multipotent progenitors (LMPPs, gated as LSK CD34$^+$Flk2$^+$)$^{-8}$ distributed among donor-derived LSKs (Lin^{neg}c-Kit$^+$Sca-1$^+$ cells). To isolate LT-HSCs, lineage depletion was performedto enrich for lineage-negative cells. Lineage-negative cells were then stained as mentioned above and sorted using a BD FACS Aria III (BD Bioscience). For intracellular flow cytometric staining of β-catenin, lineage-depleted young, aged and young plus 100 ng ml^{-1} Wnt5a bone marrow cells were incubated for 16 h in IMDM plus 10% FBS at 37°C, 5% CO_2, 3% O_2. At the end of the treatment, the

samples were moved on ice and stained again with the cocktail of biotinylated lineage antibodies. After washing, the samples were stained with anti-Sca-1 (clone D7) (eBioscience), anti-c-Kit (clone 2B8) (eBioscience), anti-CD34 (clone RAM34) (eBioscience), anti-Flk2 (clone A2F10) (eBioscience) and streptavidin (eBioscience). At the end of the surface staining, cells were fixed and permeabilized with Cytofix/ Cytoperm solution (BDBiosciences) and incubated with10% donkeyserum (Sigma) in BD Perm/Wash Buffer (BD Biosciences) for 30 min. Primary and secondary antibody incubations were performed at room temperature in BD Perm/Wash Buffer (BD Biosciences) for 1 h and 30 min, respectively. The primary antibody for β-catenin was obtained from Millipore (rabbit polyclonal). The secondary antibody is a donkey anti-rabbit DyLight649 (BioLegend). *Z*-stacks were obtained by automatically scanning along the *z* axis of the cell with a confocal microscope and acquiring a picture of the in-focus plane every 0.6 μm.

Calcium flux protocol

$Lin^{-}Sca\text{-}1^{+}c\text{-}Kit^{+}$ (LSK) cells weresorted out of 10pooled 10-week-old male C57BL/6 mice. The sorted cells were suspended in 1 ml CLM in a 15-ml tube (CLM (cell loading medium): HBSS, 1% FCS, 1 mM $CaCl_2$, 1 nM $MgCl_2$). The cells were loaded with indo-1 AM (Molecular Probes I-1203, final concentration 0.25 μM) for 45 min at 37 °C in the dark. After loading, the cells were washed twice with CLM. The indo-1 cells were then resuspended in 1 ml CLM again and stored in the dark at room temperature for 1 h. Before flow cytometric analysis, the cells were equilibrated at 37 °C in the dark for 30 min. The cells were analysed by flow cytometry. An aliquot of the untreated cells was run to establish the baseline fluorescence of the indo-1-loaded cells. In one sample, ionomycin was used aspositive control for Ca^{2+} release (1 μg ml^{-1} final concentration). After a few minutes a calcium chelator, EGTA, was added during acquisition, and served as negative (Ca^{2+} low) control (8 mM final concentration). The response to Wnt5a was measured by adding murine recombinant Wnt5a (R&D Systems) to a final concentration of 300 ng ml^{-1}, 1 min after start of the measurement. Seven minutes after the first Wnt5a addition, a second, higher concentration of Wnt5a was added (700 ng ml^{-1}). To determine the calcium response to addition of Wnt5a, indo-1-loaded LSKs were analysed relative to a time parameter, and the change in fluorescence ratio over time can be related to changes in activation or stimulation by some agonist that will elicit a calcium influx. For visualization of this influx, the change in ratio of indo-1-bound Ca^{2+} (420 nm) and free indo-1 (510 nm) was depicted against the time after start of the measurement.

Immunofluorescence staining

Freshly sorted LT-HSCs were seeded on fibronectin-coated glass coverslips. For polarity staining, LT-HSCs were incubated for 12–16 h in HBSS + 10% FBS and when indicated treated with 100 ng ml^{-1} Wnt5a (R&D System), casin (referred to in ref. 22 as Pirl1-related compound 2, obtained from Chembridge Corporation, and purified to greater than 99% by high-performance liquid chromatography) or left untreated. After incubation at 37 °C, 5% CO_2, 3% O_2, in growth factor-free medium, cells were fixed with BD Cytofix fixation buffer (BD Biosciences). After fixation cells were gently washed with PBS, permeabilized with 0.2% Triton X-100 (Sigma) in PBS for 20 min and blocked with 10% donkey serum(Sigma) for 30 min. Primary and secondary antibody incubations were performed for

1 h at room temperature. Coverslips were mounted with ProLong Gold Antifade reagent with or without DAPI (Invitrogen, Molecular Probes). The cells were stained with an anti-α-tubulin antibody (Abcam, rat monoclonal ab6160) detected with an anti-rat AMCA-conjugated secondary antibody or an anti-rat DyLight488-conjugated antibody (Jackson ImmunoResearch); an anti-Cdc42 antibody (Millipore, rabbit polyclonal) or an anti-β-catenin antibody (Millipore, rabbit polyclonal) detected with an anti-rabbit DyLight549-conjugated antibody (Jackson ImmunoResearch); an anti-pericentrin-2 antibody (Santa Cruz Biotechnology, goat polyclonal) detected with an anti-goat AMCA-conjugated antibody (Jackson ImmunoResearch); an anti-Wnt5a antibody (R&D System, goat polyclonal) detected with an anti-rat DyLight488-conjugated secondary antibody (Jackson ImmunoResearch). Samples were imaged with an AxioObserver Z1 microscope (Zeiss) equipped with a 363 PH objective. Images were analysed with AxioVision 4.6 software. Alternatively, samples were analysed with an LSM710 confocal microscope (Zeiss) equipped with a 363 objective. Primary raw data were imported into the Volocity Software package (Version 6.0, Perkin Elmer) for further processing and conversion into three-dimensional images. As for polarity scoring, the localization of each single stained protein was considered polarized when a clear asymmetric distribution was visible by drawing a line across the middle of the cell. A total of 50 to100 LT-HSCs were singularly analysed per sample. Data are plotted as percentage of the total number of cells scored per sample. Specificity of the anti-Cdc42 antibody in immunofluorescence was tested on LT-HSCs sorted from mice in which *Cdc42* was deleted specifically in the haematopoietic system (Mx1-Cre;$Cdc42^{flox/flox}$ mice[29]) (data not shown).

Immunocytofluorescence microscopy

Freshly sorted LT-HSCs were seeded on fibronectin-coated glass coverslips. LT-HSCs were incubated for 2 h in HBSS + 10% FBS and when indicated treated with 100 ng ml^{-1} *Wnt5a* (R&D System) or left untreated. After incubation at 37 °C, 5% CO_2, 3% O_2, in growth-factor-free medium cells were fixed with BD Cytofix Fixation buffer (BD Biosciences). Cells were incubated with primary antibodies diluted in blocking buffer overnight at 4 °C. Cells were then washed three times with PBS and incubated with a secondary antibody diluted 1:1,000 in blocking buffer overnight at 4 °C. The primary and secondary antibodies used were: anti-CamkII (polyclonal rabbit, Cell Signaling Technology), phosphor-Thr 286-CamkII (polyclonal rabbit, Cell Signaling Technology), and anti-NFATc1 (mouse monoclonal IgG1, clone 7A6, Santa Cruz Biotechnology). After final washes, the coverslips were mounted in SlowFade Gold Antifade reagent supplemented with DAPI (4,6-diamino-2-phenylindole,dihydro-chloride) nuclear stain (Invitrogen). Fluorescence digital images were taken using constant settings on a Leica DM RBE fluorescent microscope (Leica) using AxioVision software (Carl Zeiss). For each particular sample, images at ×100 magnification of between 30 and 100 randomly captured cells were taken. Fluorescence digital images were then analysed using the digital image processing software ImageJ (NIH). The mean fluorescence intensity (average intensity of pixels per cell) was determined. Background correction was performed by determining the signal intensity of the pixels around the perimeter of the area being quantified. These background signals were then subtracted from specific signals caused by antibody staining. To compare measurements from separate experiments, they were additionally normalized to the mean of a set of control samples and

expressed as fold changes in relation to the control samples. For comparison of means of different groups, a two-tailed *t*-test assuming equal variances was used. A *P* value less than 0.05 was considered to be statistically significant.

Western blot and Cdc42-GTPase effector domain pull-down assays

Relative levels of GTP-bound Cdc42 were determined by an effector pull-down assay. Briefly, lineage-depleted bone-marrow cells (10^6) were lysed in a Mg^{2+} lysis/wash buffer (Upstate cell signalling solutions) containing 10% glycerol, 25 mM sodium fluoride, 1 mM sodium orthovanadate and a protease inhibitor cocktail (Roche Diagnostics). Samples were incubated with PAK-1 binding domain/agarose beads and bound (activated) as well as unbound (non-activated) Cdc42 fractions were probed by immunoblotting with an anti-Cdc42 antibody (Millipore, rabbit polyclonal). Activated protein was normalized to total protein and/or β-actin (Sigma) and the relative amount was quantified by densitometry. For detection of Wnt5a protein levels, cells were lysed as mentioned above and directly blotted with a goat anti-mouse Wnt5a antibody (R&D Systems). Wnt5a protein levels were normalized based on actin protein levels in the same blotted samples.

Reverse-transcriptase real-time PCR

20,000–40,000 LT-HSCs from young and aged mice were lysed and processed for RNA extraction immediately after sorting. RNA was obtained with the microRNA Extraction kit (Qiagen) and all was used for cDNA conversion. cDNA was prepared and amplified with Ovation RNA Amplification system V2 (NuGEN). All real-time PCRs were run with TaqMan real-time PCR reagent and primers from Applied Biosystem on an ABI9700HT real time machine.

Stroma $CD45^-$ cells

To isolate cells close to the endosteum, femora and tibiae were isolated from young (2–3-month-old) and aged (22–23-month-old) mice. The bones were cleaned and the associated muscle tissues removed. After the bone marrow was flushed, the bones were crushed using scissors and minced with a scalpel in 1.5 mg ml^{-1} collagenase IV (Worthington)/PBS. The bone chips were further incubated and shaken for 1.5 h at 37 °C in collagenase IV/PBS. The bone chips were washed extensively with IMDM/10%FBS and the dissociated cells collected. This stroma cell fraction was filtered through a 100 μm cell strainer and stained for with an anti-CD45 antibody (clone 104), and CD45 negative cells sorted by flow cytometry.

shRNA lentiviral transduction

Aged mice (24-month-old) were killed; bone marrow mononuclear cells were isolated by low-density centrifugation (Histopaque 1083, Sigma) and stained with a cocktail of biotinylated lineage antibodies. Biotinylated antibodies used for lineage staining were all rat anti-mouse antibodies: anti-CD11b (clone M1/70), anti-B220 (clone RA3-6B2), anti-CD5 (clone 53-7.3) anti-Gr-1 (clone RB6-8C5), anti-Ter119 and anti-CD8a (clone 53-6.7) (all from eBioscience).Not pre-stimulated, aged, lineage-depleted bone marrow cells (Lin^-BM) were transduced overnight on retronectin-coated (TaKaRa) plates with cell-free supernatants

containing lentiviral particles according to refs 30, 31. The lentivirus plasmid vector pLKO.1-YFP was obtained from Sigma's validated genome-wide TRC shRNA libraries (Sigma-Aldrich).

Statistical analyses

Data were assumed to meet normal distribution. The variance was similar between groups that were statistically compared. All data are plotted as mean + 1 standard error (s.e.m.) unless differently stated. The s.e.m. is used to indicate the precision of an estimated mean. Such a data representation does not affect the statistical analyses as variance information is used in the test statistics. A paired Student's *t*-test was used to determine the significance of the difference between means of two groups. One-way ANOVA or two-way ANOVA were used to compare means among three or more independent groups. Bonferroni post-test to compare all pairs of data set was determined when overall P value was <0.05. All statistical analyses were determined with Prism 4.0c version. To choose sample size, we used GraphPad StatMate Software Version 2.0b, estimating a standard deviation between 2 and 8 (depending on the experiment and the possibility of increasing sample size). For transplantation experiments we estimated a sample size of 15–20 (assuming a standard deviation of 10 and a significant difference between means of at least 15). In transplantation experiments, samples were included in the analysis when engraftment was more or equal to 1.0% after at least 12 weeks from injections (24 weeks for most of the experiments) and contribution was detected in all lineages. Mice showing signs of sickness and with clear alterations of blood parameter and/or showing signs of major disease involving also non-haematopoietic tissues were excluded from analysis. As for *in vitro* experiments, samples were excluded from analysis in case of clear technical problems (error in immune-blotting or staining procedures or technical problems with reagents). All criteria for exclusions of samples from *in vivo* or *in vitro* experiments were pre-established. In each figure legend, the number (n) of biological repeats (samples obtained from experiments repeated in different days and starting from different mice) included in the final statistical analysis is indicated. Mice for experiments were randomly chosen from our in-house colonies or suppliers. All mice were C57BL/6 females unless differently stated. The investigator was not blinded to the mouse group allocation nor when assessing the outcome (aged mice or young mice transplanted with aged bone marrow stem cells require particular care and follow up).

Supplementary Material

Refer to Web version on PubMed Central for supplementary material.

Acknowledgments

We thank G. Van Zant and J. A. Cancelas for advice and critical reading of the manuscript. We thank F. Kirchhoff and D. van der Merwe for cell sorting support, A. Rück and the Institut für Lasertechnologien in der Medizin und Meßtechnik of Ulm University for support with confocal microscopy, and the Mouse and Cancer Core in Cincinnati and the Tierforschungszentrum of the University of Ulm for supporting our animal work. The work in the laboratory of H.G. is supported by grants from the Deutsche Forschungsgemeinschaft KFO 142, GE2063/1 and SFB 1074, the German Federal Ministry of Education and Research within its joint research project SyStaR (also to H.A.K. and K.S.-K.), the Excellence program of the Baden-Württemberg Foundation, the National Institute of Health, HL076604, DK077762 and AG040118, the Edward P. Evans foundation and the European Commission (FP7 Marie Curie Initial Training Network MARRIAGE). M.C.F. is supported by a ‘Bausteinprogramm’ of the Department of Medicine of Ulm University.

References

1. Morrison SJ, Uchida N, Weissman IL. The biology of hematopoieticstem cells. Annu. Rev. Cell Dev. Biol. 1995; 11:35–71. [PubMed: 8689561]
2. Fuchs E, Segre JA. Stem cells: a new lease on life. Cell. 2000; 100:143–155. [PubMed: 10647939]
3. Rossi DJ, et al. Cell intrinsic alterations underlie hematopoietic stem cell aging. Proc. Natl Acad. Sci. USA. 2005; 102:9194–9199. [PubMed: 15967997]
4. Rossi DJ, Jamieson CH, Weissman IL. Stems cells and the pathways to aging and cancer. Cell. 2008; 132:681–696. [PubMed: 18295583]
5. Geiger H, Van Zant G. The aging of lympho-hematopoietic stem cells. Nature Immunol. 2002; 3:329–333. [PubMed: 11919569]
6. Geiger H, Rudolph KL. Aging in the lympho-hematopoietic stem cell compartment. Trends Immunol. 2009; 30:360–365. [PubMed: 19540806]
7. Conboy IM, Conboy MJ, Smythe GM, Rando TA. Notch-mediated restoration of regenerative potential to aged muscle. Science. 2003; 302:1575–1577. [PubMed: 14645852]
8. Conboy IM, et al. Rejuvenation of aged progenitor cells by exposure to a young systemic environment. Nature. 2005; 433:760–764. [PubMed: 15716955]
9. Brack AS, et al. Increased Wnt signaling during aging alters muscle stem cell fate and increases fibrosis. Science. 2007; 317:807–810. [PubMed: 17690295]
10. Liu H, et al. Augmented Wnt signaling in a mammalian model of accelerated aging. Science. 2007; 317:803–806. [PubMed: 17690294]
11. Malhotra S, Kincade PW. Wnt-related molecules and signaling pathway equilibrium in hematopoiesis. Cell Stem Cell. 2009; 4:27–36. [PubMed: 19128790]
12. Nemeth MJ, Topol L, Anderson SM, Yang Y, Bodine DM. Wnt5a inhibits canonical Wnt signaling in hematopoietic stem cells and enhances repopulation. Proc. Natl Acad. Sci. USA. 2007; 104:15436–15441. [PubMed: 17881570]
13. Duncan AW, et al. Integration of Notch and Wnt signaling in hematopoietic stem cell maintenance. Nature Immunol. 2005; 6:314–322. [PubMed: 15665828]
14. Luis TC, Naber BA, Fibbe WE, van Dongen JJ, Staal FJ. Wnt3a nonredundantly controls hematopoietic stem cell function and its deficiency results in complete absence of canonical Wnt signaling. Blood. 2010; 116:496–497. [PubMed: 20651084]
15. Luis TC, et al. Canonical Wnt signaling regulates hematopoiesis in a dosage-dependent fashion. Cell Stem Cell. 2011; 9:345–356. [PubMed: 21982234]
16. Staal FJ, Luis TC. Wnt signaling in hematopoiesis: crucial factors for self-renewal, proliferation, and cell fate decisions. J. Cell. Biochem. 2010; 109:844–849. [PubMed: 20069555]
17. Schlessinger K, Hall A, Tolwinski N. Wnt signaling pathways meet Rho GTPases. Genes Dev. 2009; 23:265–277. [PubMed: 19204114]
18. Schlessinger K, McManus EJ, Hall A. Cdc42 and noncanonical Wnt signal transduction pathways cooperate to promote cell polarity. J. Cell Biol. 2007; 178:355–361. [PubMed: 17646398]
19. Sugimura R, et al. Noncanonical Wnt signaling maintains hematopoietic stem cells in the niche. Cell. 2012; 150:351–365. [PubMed: 22817897]
20. Florian MC, et al. Cdc42 activity regulates hematopoietic stem cell aging and rejuvenation. Cell Stem Cell. 2012; 10:520–530. [PubMed: 22560076]
21. Geiger H, de Haan G, Florian MC. The ageing haematopoietic stem cell compartment. Nature Rev. Immunol. 2013; 13:376–389. [PubMed: 23584423]
22. Peterson JR, Lebensohn AM, Pelish HE, Kirschner MW. Biochemical suppression of small-molecule inhibitors: a strategy to identify inhibitor targets and signaling pathway components. Chem. Biol. 2006; 13:443–452. [PubMed: 16632257]
23. Liang H, et al. Wnt5a inhibits B cell proliferation and functions as a tumor suppressor in hematopoietic tissue. Cancer Cell. 2003; 4:349–360. [PubMed: 14667502]
24. Kuhl M, Sheldahl LC, Park M, Miller JR, Moon RT. The Wnt/Ca^{21} pathway: a new vertebrate Wnt signaling pathway takes shape. Trends Genet. 2000; 16:279–283. [PubMed: 10858654]

25. Zou P, et al. $p57^{Kip2}$ and $p27^{Kip1}$ cooperate to maintain hematopoietic stem cell quiescence through interactions with Hsc70. Cell Stem Cell. 2011; 9:247–261. [PubMed: 21885020]
26. Li J, et al. WNT5A antagonizes WNT/β-catenin signaling and is frequently silenced by promoter CpG methylation in esophageal squamous cell carcinoma. Cancer Biol. Ther. 2010; 10:617–624. [PubMed: 20603606]
27. Kohler A, et al. Altered cellular dynamics and endosteal location of aged early hematopoietic progenitor cells revealed by time-lapse intravital imaging in long bones. Blood. 2009; 114:290–298. [PubMed: 19357397]
28. Adolfsson J, et al. Identification of $Flt3^{+}$ lympho-myeloid stem cells lacking erythro-megakaryocytic potential a revised road map for adult blood lineage commitment. Cell. 2005; 121:295–306. [PubMed: 15851035]
29. Yang L, et al. Cdc42 critically regulates the balance between myelopoiesis and erythropoiesis. Blood. 2007; 110:3853–3861. [PubMed: 17702896]
30. Daria D, et al. The retinoblastoma tumor suppressor is a critical intrinsic regulator for hematopoietic stem and progenitor cells under stress. Blood. 2008; 111:1894–1902. [PubMed: 18048646]
31. Li Z, et al. Predictable and efficient retroviral gene transfer into murine bone marrow repopulating cells using a defined vector dose. Exp. Hematol. 2003; 31:1206–1214. [PubMed: 14662326]

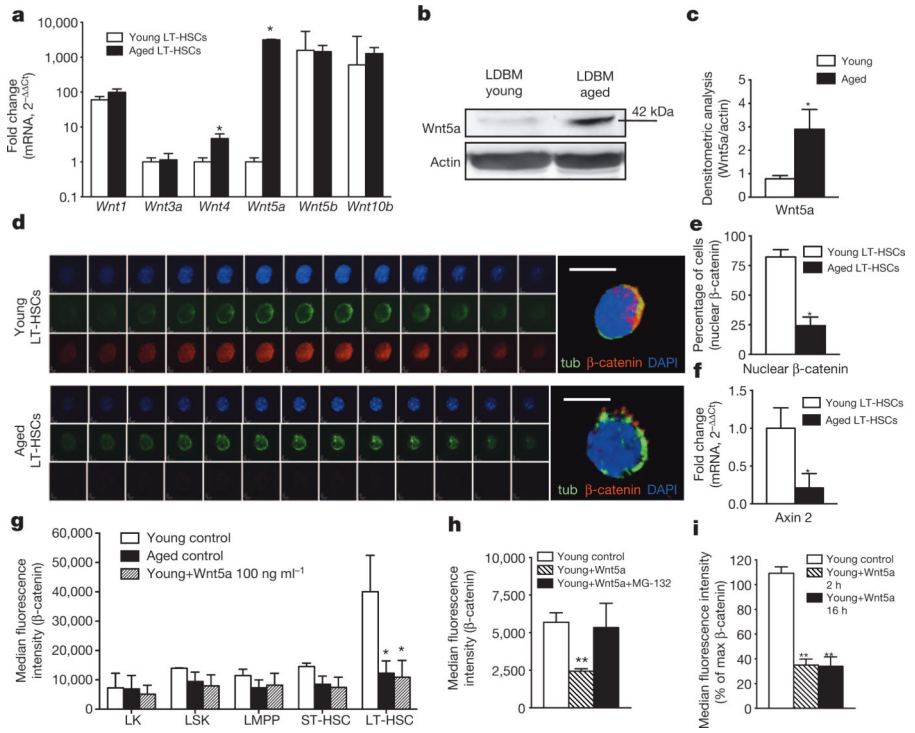

Figure 1. Increased expression of Wnt5a in aged LT-HSCs results in a shift from canonical to non-canonical Wnt signalling

a, Wnt transcript levels in 2–3-month-old or 24-month-old LT-HSCs. $n = 4$, $^*P < 0.05$. **b, c,** Wnt5a protein levels in low-density bone marrow (LDBM) cells (b) and densitometric score (c). $n = 4$, $^*P < 0.05$. **d,** Immunofluorescence *z*-stack and three-dimensional merged images of tubulin (green) and β-catenin (red) in LT-HSCs. Scale bar, 5 μm. **e,** LT-HSCs with nuclear β-catenin. $n = 3$, 200 cells per sample in total. $^*P < 0.05$. **f,** Axin 2 transcript levels in LT-HSCs. $n = 4$, $^*P < 0.05$. **g,** β-catenin mean fluorescence intensity in young, aged and young Wnt5a-treated haematopoietic progenitor/stem cells. $n = 3$, $^*P < 0.05$ versus young LT-HSC controls. **h,** β-catenin mean fluorescence intensity in young control LT-HSCs, or young LT-HSCs treated with Wnt5a or with Wnt5a plus MG-132. $n = 3$, $^{**}P < 0.01$ versus young controls. **i,** β-catenin mean fluorescence intensity in young LT-HSCs or young LT-HSCs treated with Wnt5a. $n = 3$, $^{**}P < 0.01$ versus young controls. A paired Student's *t*-test was used to determine the significance of the difference between means of two groups. One-way ANOVA or two-way ANOVA were used to compare means among three or more independent groups. Error bars represent s.e.m.

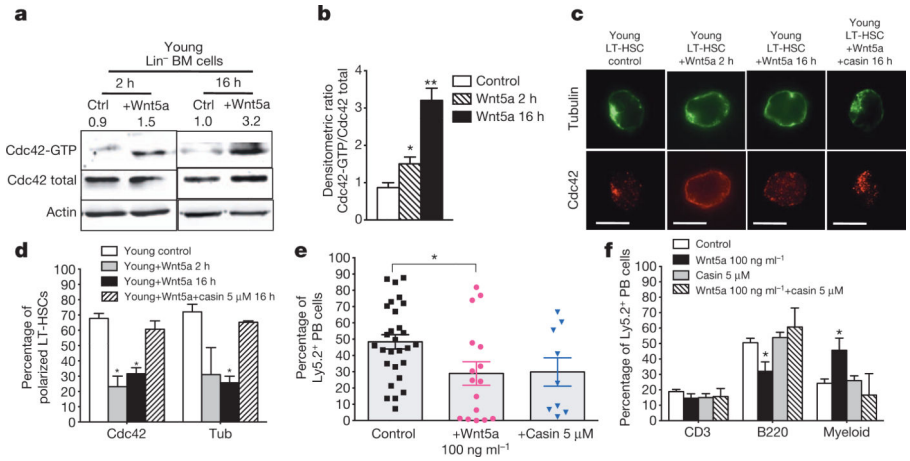

Figure 2. Wnt5a activates Cdc42 inducing ageing-like phenotypes in young LT-HSCs

a, b, Cdc42 activity in young and Wnt5a-treated Lin$^-$ bone marrow (BM) cells (**a**) and densitometric score (**b**). $n = 4$, $^*P < 0.05$, $^{**}P < 0.01$. **c**, Cdc42 (red) and tubulin (green) in LT-HSCs shown by immunofluorescence. Scale bar, 5 μm. **d,** Polar distribution (percentage) of Cdc42 and tubulin in LTHSCs. $n = 6$, 200 LT-HSCs per sample in total. $^*P < 0.001$. **e, f,** Donor-derived Ly5.2$^+$ cells and B220$^+$, CD3$^+$ and myeloid (Gr1$^+$, Mac1$^+$, Gr1$^+$Mac1$^+$) cells among Ly5.2$^+$ cells in peripheral blood (PB) 24 weeks after transplant. $^*P < 0.05$; $n = 10$ for casin and Wnt5a plus casin, $n = 25$ for control and Wnt5a. A paired Student's *t*-test was used to determine the significance of the difference between means of two groups. One-way ANOVA or two-way ANOVA were used to compare means among three or more independent groups. Error bars represent s.e.m.

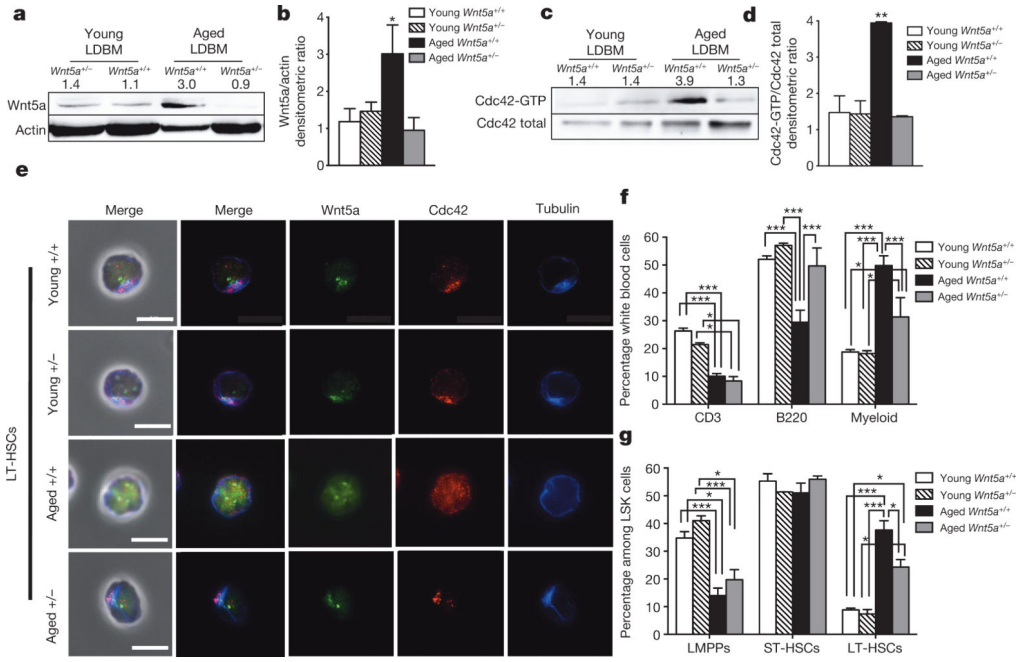

Figure 3. Wnt5a haploinsufficient mice present with attenuated HSC ageing

a–d, Wnt5a (**a**) and Cdc42 activity levels (**c**) in young and aged *Wnt5a*$^{+/+}$ and *Wnt5a*$^{+/-}$ LDBM cells and densitometric analysis (**b, d**). $n = 4$, $^{*}P < 0.05$; $^{**}P < 0.01$. **e,** Distribution of Cdc42, tubulin and *Wnt5a* in young and aged *Wnt5a*$^{+/+}$ and *Wnt5a*$^{+/-}$ LT-HSCs. Scale bar, 5 μm. **f, g,** Percentage of B220^{+}, CD3^{+} and myeloid cells among white blood cells in peripheral blood (**f**) and percentage of LT-HSCs, ST-HSCs and LMPPs among LSKs (**g**) in *Wnt5a*$^{+/+}$ and *Wnt5a*$^{+/-}$ young and aged mice. $^{*}P < 0.05$, $^{**}P < 0.01$, $^{***}P < 0.001$; $n = 5$ for aged *Wnt5a*$^{+/+}$ and *Wnt5a*$^{+/-}$ mice; $n = 7$ for young *Wnt5a*$^{+/+}$ and *Wnt5a*$^{+/-}$ mice. A paired Student's *t*-test was used to determine the significance of the difference between means of two groups. One-way ANOVA or two-way ANOVA were used to compare means among three or more independent groups. Error bars represent s.e.m.

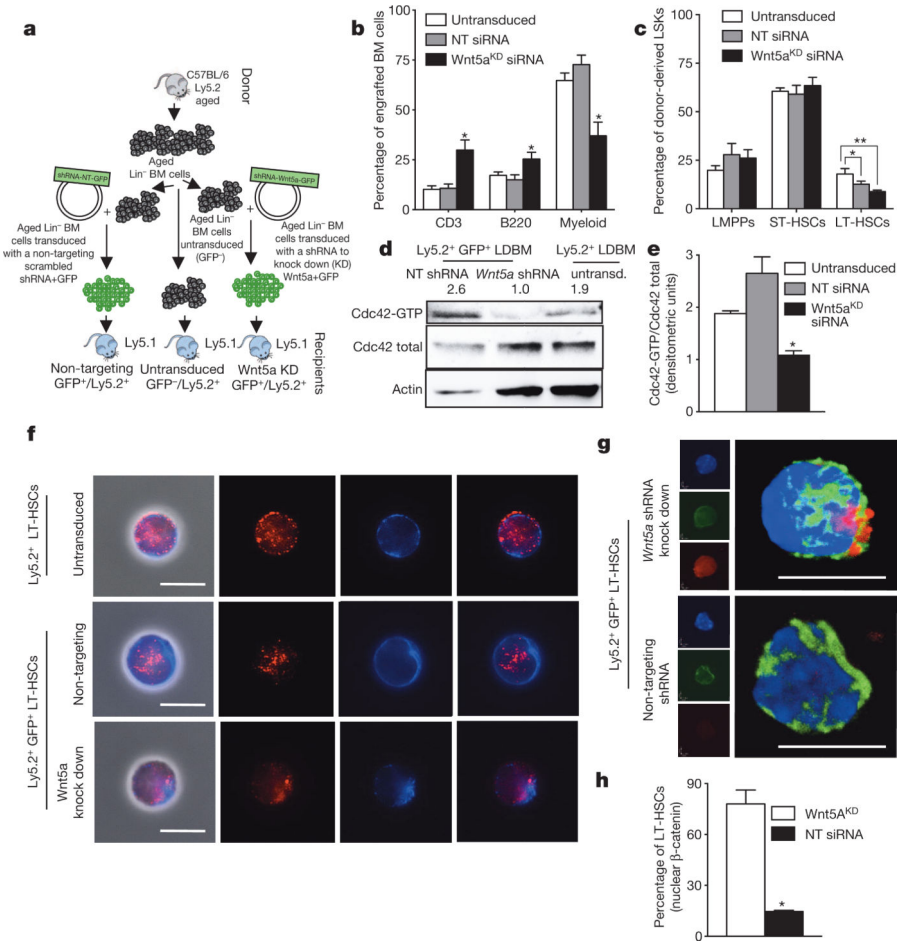

Figure 4. Reducing Wnt5a expression in aged LT-HSCs rejuvenates their function *in vivo*

a, Experimental set-up. **b,** $B220^+$, $CD3^+$ and myeloid cells among donor-derived cells in bone marrow. $*P < 0.05$; $n = 10$. **c,** LT-HSCs, ST-HSCs and LMPPs among donor-derived LSKs. $*P < 0.05$; $**P < 0.01$. **d, e,** Cdc42 activity in aged donor-derived low-density bone-marrow (LDBM) cells transduced with non-targeting (NT) shRNA, *Wnt5a* shRNA ($Wnt5a^{KD}$) and untransduced control (**d**) and densitometric score (**e**). $n = 4$, $*P < 0.05$. **f,** Cdc42 and tubulin in donor-derived LT-HSCs from aged untransduced or non-targeting shRNA or $Wnt5a^{KD}$ recipient mice 24 weeks after transplant shown by immunofluorescence. Scale bar, 5 μm. **g,** Immunofluorescence *z*-stack and three-dimensional merged images of tubulin (green) and β-catenin (red) localization in aged non-targeting shRNA or $Wnt5a^{KD}$ LT-HSCs. Scale bar, 5 μm. **h,** Aged donor-derived non-targeting shRNA or $Wnt5a^{KD}$ LT-HSCs exhibiting nuclear accumulation of β-catenin. $n = 3$, $*P < 0.05$. A paired Student's *t*-test was used to determine the significance of the difference between means of two groups. One-way ANOVA or two-way ANOVA were used to compare means among three or more independent groups. Error bars represent s.e.m.

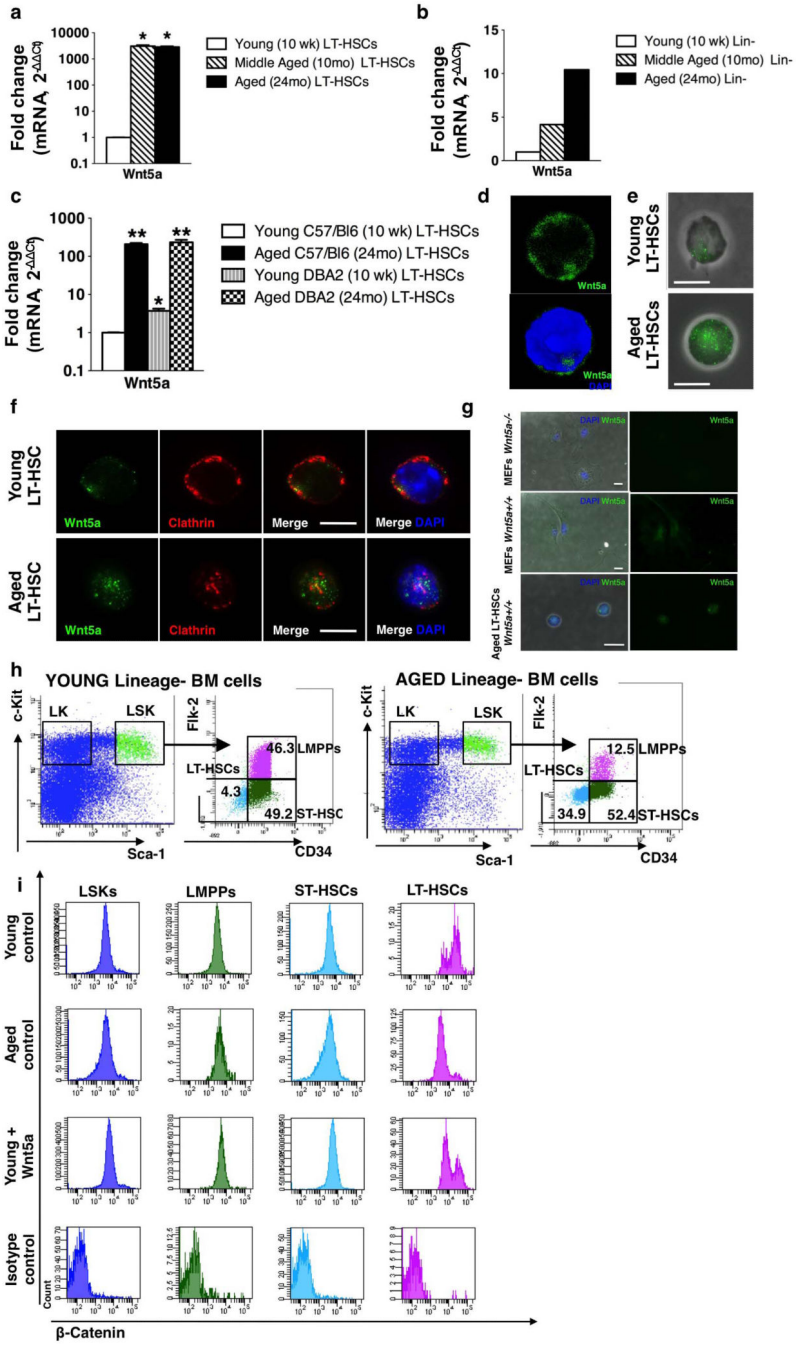

Extended Data Figure 1. Increased expression of Wnt5a in aged LT-HSCs results in a shift from canonical to non-canonical Wnt signalling

a, Reverse transcriptase real-time PCR analysis of *Wnt5a* transcript levels in young (10-week-old), middle-aged (10-month-old) and aged (24-month-old) LT-HSCs ($Lin^{-}c\text{-}kit^{+}Sca\text{-}1^{+}Flk2^{-}CD34^{-}$ bone marrow cells) sorted from C57BL/6 mice. Data are expressed as fold increased compared to the lowest expressed transcript arbitrarily set to 1. *Wnt5a* mRNA is barely detectable in young LT-HSCs and is markedly upregulated in middle-aged and aged LT-HSCs. Data were analysed with the $2^{-\Delta\Delta Ct}$ method and plotted on a

logarithmic scale. Bars are mean + 1 s.e.; $n = 3$, $^{*}P < 0.05$. **b,** Reverse transcriptase real-time PCR analysis of *Wnt5a* transcript levels in young (10-week-old), middle-aged (10-month-old) and aged (24-month-old) Lin^{-} bone marrow cells from C57BL/6 mice. Data are expressed as fold increased compared to the lowest expressed transcript arbitrarily set to 1. *Wnt5a* mRNA is barely detectable in young Lin^{-} cells and is upregulated in middle-aged and aged LT-HSCs. Data were analysed with the $2^{-\Delta\Delta Ct}$ method and plotted on a logarithmic scale. Scale bars represent results of one set of samples. The experiment was repeated twice with similar results. **c,** Reverse transcriptase real-time PCR analysis of *Wnt5a* transcript levels in young (10-week-old) and aged (24-month-old) LT-HSCs (Lin^{-}c-$Kit^{+}Sca\text{-}1^{+}Flk2^{-}CD34^{-}$ bone marrow cells) sorted from C57BL/6 and DBA/2 mice. Data are expressed as fold increased compared to the lowest expressed transcript arbitrarily set to 1. Data were analysed with the $2^{-\Delta\Delta Ct}$ method and plotted on a logarithmic scale. Error bars are mean + 1 s.e.; $n = 3$, $^{*}P < 0.05$, $^{**}P < 0.01$. **d,** Representative three-dimensional confocal picture of *Wnt5a* distribution in an aged LT-HSC. The nucleus is stained with DAPI. Three-dimensional localization of Wnt5a was analysed by scanning the cells along the *z*-axis and acquiring a picture of the *xy*-plane every 0.7 μm. Three-dimensional images were then reconstructed by using Volocity v6.0 software. **e,** Representative immunofluorescence picture of Wnt5a (green) membrane distribution (non-permeabilized cells) in young and aged LT-HSCs. Immunofluorescence pictures are shown as overlap with the phase contrast image. Scale bar, 5 μm. **f,** Representative immunofluorescence picture of Wnt5a (green) and clathrin (red) localization in young and aged LT-HSCs. Pictures are shown on a dark background and as overlap with DAPI (staining nuclei). Scale bar, 5 μm. **g,** Representative expression of Wnt5a in MEFs (mouse embryonic fibroblasts) and aged LT-HSCs from $Wnt5a^{+/+}$ mice determined by immunofluorescence. Wnt5a fluorescence signal is not detected when MEFs from $Wnt5a^{-/-}$ mice are stained with the same procedure. Wnt5a pictures are shown on a dark background and as overlap with DAPI (blue, staining nuclei) and phase contrast images. Scale bar, 10 μm. **h,** Representative FACS dot plots of LT-HSCs (Lin^{-}c-$Kit^{+}Sca\text{-}1^{+}Flk2^{-}CD34^{-}$), ST-HSCs ($Lin^{-}$c-$Kit^{+}Sca\text{-}1^{+}Flk2^{-}CD34^{+}$), LMPPs ($Lin^{-}$c-$Kit^{+}Sca\text{-}1^{+}Flk2^{+}CD34^{+}$), LSKs ($Lin^{-}$c-$Kit^{+}Sca\text{-}1^{+}$) and LKs ($Lin^{-}$c-$Kit^{+}Sca\text{-}1^{-}$) gating strategy of young and aged lineage-depleted bone marrow cells. **i,** Representative FACS histograms of β-catenin expression in young, aged and young *Wnt5a*-treated LT-HSCs, ST-HSCs, LMPPs and LSKs.

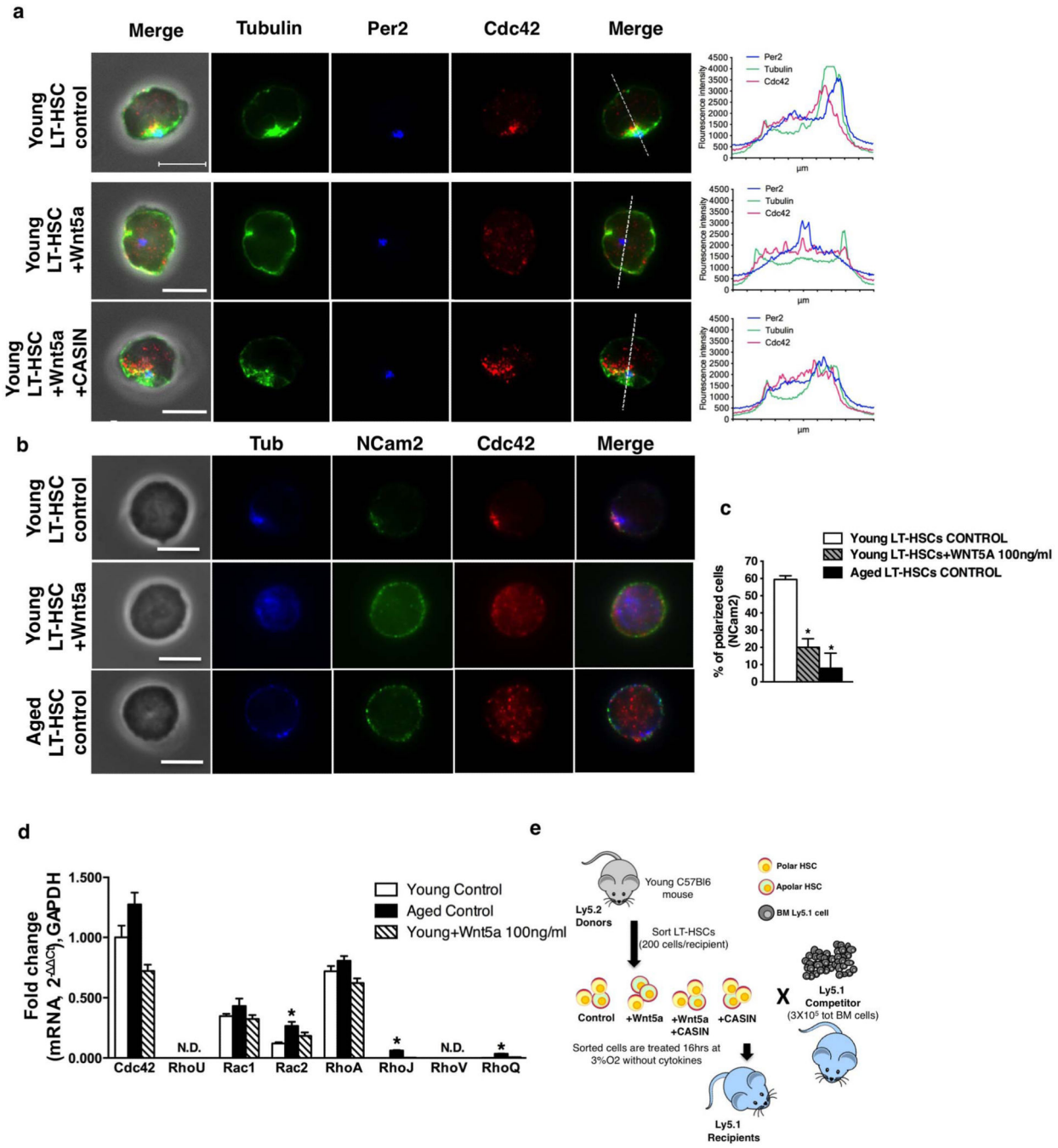

Extended Data Figure 2. Wnt5a activates Cdc42 inducing ageing-like phenotypes in young LT-HSCs

a, Representative distribution of Cdc42, tubulin and Per2 (staining the centrosome) in young control, young *Wnt5a*-treated (100 ng ml^{-1}) and young Wnt5a (100 ng ml^{-1}) 1 casin (5 µM)-treated LT-HSCs determined by immunofluorescence. Scale bar, 5 µm. Shown are also representative fluorescence intensity plots obtained by collecting pixel intensity through the section of the cell as indicated by the dotted line in the corresponding merge picture. **b,** Representative distribution of Cdc42, tubulin and NCam2 (membrane protein) in young control, young Wnt5a-treated (100 ng ml^{-1}) and aged LT-HSCs determined by

immunofluorescence. Scale bar, 5 μm. **c,** Graph of the percentage of young control, young Wnt5a-treated (100 ng ml^{-1}) and aged LT-HSCs with a polar distribution of NCam2. Shown are mean + 1 s.e., $n = 4$; ~200–300 LT-HSCs scored per sample in total. *$P < 0.001$. **d,** Reverse transcriptase real-time PCR analysis of *Cdc42*, *Rhou*, *Rac1*, *Rac2*, *Rhoa*, *Rhoj*, *Rhov* and *Rhoq* transcript levels in young, aged and young Wnt5a-treated (100 ng ml^{-1}, 16 h treatment) LT-HSCs. *Rhou* and *Rhov* transcripts were below detection limits in all the assayed samples (ND). Data are expressed as fold difference compared to the expression of *Cdc42* mRNA in young LT-HSCs arbitrarily set to 1. Data were analysed with the $2^{-\Delta\Delta Ct}$ method and plotted on a linear scale. Bars are mean + 1 s.e.; $n = 3$, *$P < 0.05$. **e,** Schematic representation of the experimental set-up for the transplantation. Recipient mice were analysed 24 weeks after transplant.

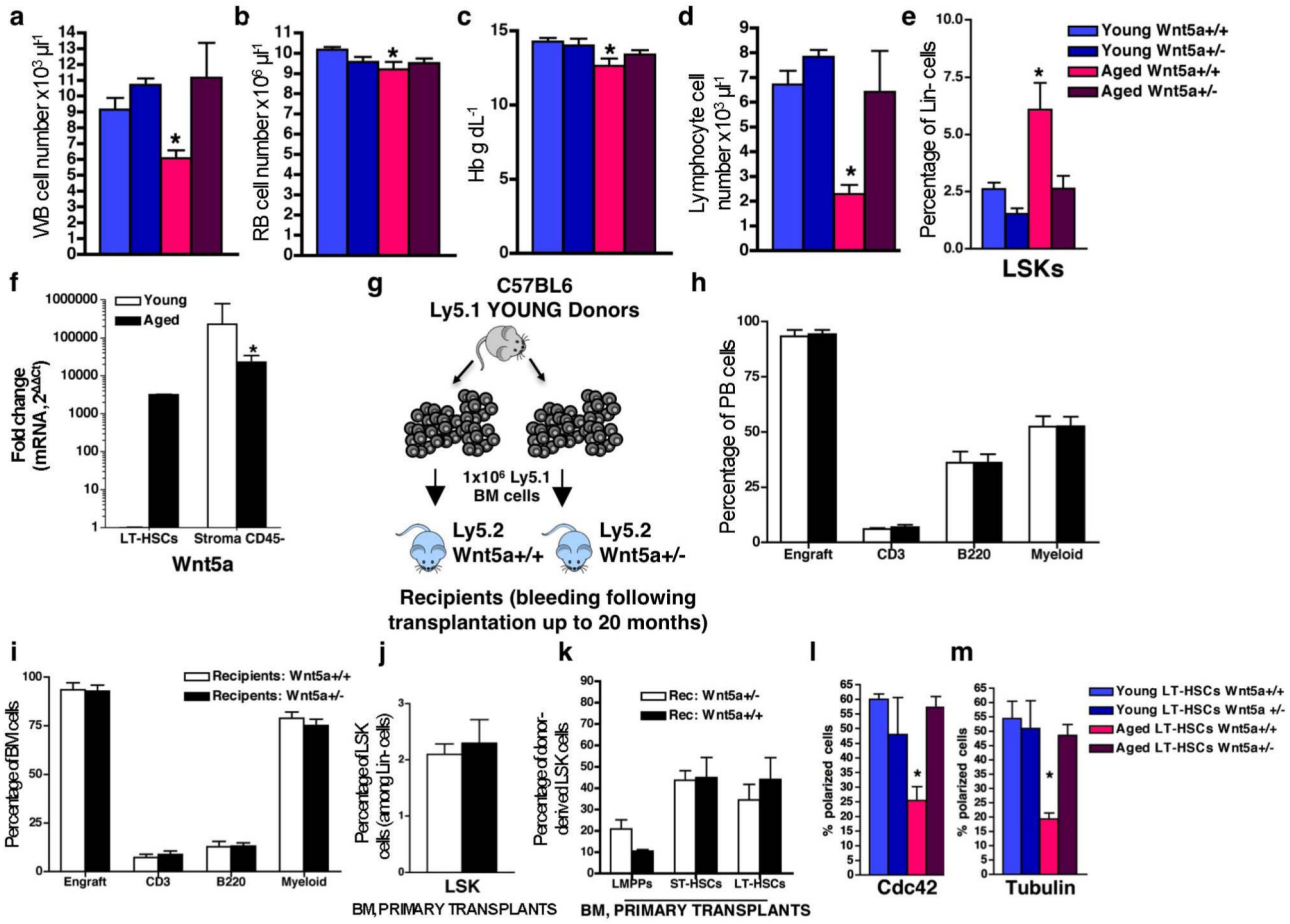

Extended Data Figure 3. Wnt5a haploinsufficient mice present with attenuated HSC ageing

a–d, White blood (WB) cell count (**a**), red blood (RB) cell count (**b**), haemoglobin (Hb) dosage (**c**) and lymphocyte cell count (**d**) in peripheral blood of young and aged *Wnt5a*$^{+/-}$ and *Wnt5a*$^{+/+}$ mice. *$P < 0.05$; shown are mean + 1 s.e., $n = 5$. **e,** Percentage of LSKs among Lin$^-$ cells in bone marrow of young and aged *Wnt5a*$^{+/-}$ and *Wnt5a*$^{+/+}$ mice. *$P < 0.05$; shown are mean + 1 s.e., $n = 5$. **f,** Reverse transcriptase real-time PCR analysis of *Wnt5a* transcript levels in young and aged LT-HSCs and young and aged collagenase-digested and sorted CD45$^-$ cells (stroma cells). Data are expressed as fold difference compared to the expression in young LT-HSCs arbitrarily set to 1. *Wnt5a* mRNA shows significantly increased expression in stroma CD45$^-$ cells when compared to young and aged LT-HSCs. In contrast to the situation in LT-HSCs, young stroma CD45$^-$ cells express higher levels of *Wnt5a* mRNA than aged stroma CD45$^-$ cells. Data were analysed with the $2^{-\Delta\Delta Ct}$ method and plotted on a logarithmic scale. Error bars are mean + 1 s.e.; $n = 4$, *$P < 0.05$. **g,** Schematic representation of the experimental set-up for transplantation. Young donor (Ly5.1$^+$) bone marrow cells were transplanted into recipient (Ly5.2$^+$) young *Wnt5a*$^{+/-}$ and *Wnt5a*$^{+/+}$ mice. Recipient mice were killed and analysed 20 months after transplant. **h, i,** Percentage of engrafted cells, B220$^+$, CD3$^+$ and myeloid cells among donor-derived Ly5.1$^+$ cells in peripheral blood (**h**) and bone marrow (**i**) 20 months after transplants. Columns are mean values + 1 s.e., $n = 5$. **j,** Percentage of donor-derived LSKs among donor-derived Lin$^-$

cells in bone marrow of *Wnt5a*$^{+/-}$ and *Wnt5a*$^{+/+}$ recipient mice 20 months after transplant. Columns show mean + 1 s.e.m., $n = 5$. **k,** Percentage of donor-derived LT-HSCs, ST-HSCs and LMPPs among donor-derived LSKs in *Wnt5a*$^{+/-}$ and *Wnt5a*$^{+/+}$ recipient mice 20 months after transplant. Columns are mean values + 1 s.e. $n = 5$. **l, m,** Percentage of LT-HSCs polarized for Cdc42 (**l**) and tubulin (**m**) in young and aged *Wnt5a*$^{+/+}$ and *Wnt5a*$^{+/-}$ mice. Shown are mean + 1 s.e., $n = 4$ and 200 cells scored per sample in total. *$P < 0.01$ versus young *Wnt5a*$^{+/+}$ and $P < 0.05$ versus young *Wnt5a*$^{+/-}$ and aged *Wnt5a*$^{+/-}$ mice.

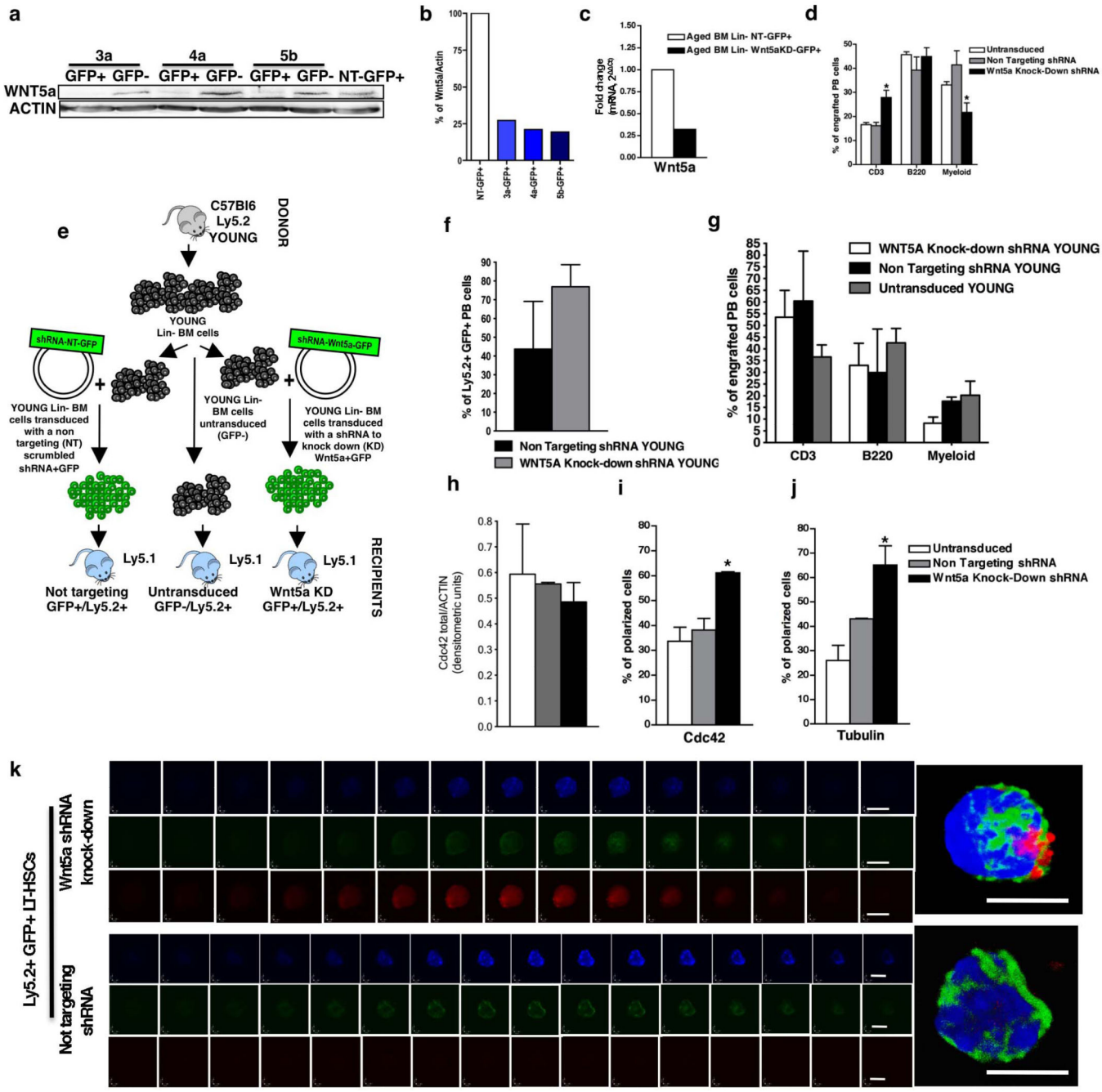

Extended Data Figure 4. Validation of the knockdown efficiency in 3T3 fibroblast cells and aged and young Lin$^-$ bone marrow cells

a, Transduced fibroblast cells were sorted and analysed by western blot for *Wnt5a* protein levels. Wnt5a protein levels were normalized on actin. Three different Wnt5a knockdown vectors (3a-GFP$^+$, 4a-GFP$^+$, 5b-GFP$^+$) were tested and Wnt5a protein levels were compared to non-targeting transduced fibroblasts (NT-GFP$^+$) and to untransduced cells sorted as GFP$^-$ from the initial mixed culture (3a-GFP$^-$, 4a-GFP$^-$, 5b-GFP$^-$). **b,** Transduced fibroblast cells were sorted and analysed by reverse transcriptase real-time PCR for *Wnt5a* mRNA levels. *Wnt5a* mRNA levels are normalized to actin mRNA levels. Three different Wnt5a

knockdown vectors (3a-GFP$^+$, 4a-GFP$^+$, 5b-GFP$^+$) were tested and *Wnt5a* transcript levels were compared to non-targeting transduced fibroblasts (NT-GFP$^+$). **c,** Not pre-stimulated transduced *Wnt5a*^{KD} or non-targeted aged Lin$^-$ bone marrow cells were sorted and analysed by reverse transcriptase real-time PCR for *Wnt5a* mRNA levels. *Wnt5a* mRNA levels are normalized on *Gapdh* mRNA levels. **d,** Percentage of B220$^+$, CD3$^+$ and myeloid cells among donor-derived cells in peripheral blood 24 weeks after transplant. *$P < 0.05$; shown are mean values + 1 s.e. Mice were considered as engrafted when the percentage of Ly5.2$^+$ cells in peripheral blood was higher than 1.0 and contribution was detected for all peripheral blood lineages. Data are based on two different lentiviral infection/transplant experiments with 5–7 recipient mice per group (for example, $n = 10$). **e,** Schematic representation of the experimental set-up for transplantation of Wnt5a knock down (Wnt5a^{KD}), Wnt5a non-targeting (Wnt5a-NT) and untransduced young haematopoietic progenitor/stem cells. Young donor (Ly5.2$^+$) lineage-negative (Lin$^-$) bone marrow cells were infected with the indicated lentiviral vectors or left untransduced. Infected cells were sorted based on GFP expression. Cells (1–3 × 10^5 Ly5.2$^+$) were transplanted into recipients (Ly5.1$^+$). Recipient mice were analysed 12–16 weeks after transplant. **f,** Percentage of engrafted donor-derived cells in peripheral blood 12–16 weeks after transplant. Shown are mean values + 1 s.e. Mice were considered as engrafted when the percentage of Ly5.2$^+$ cells in peripheral blood was higher than 1.0 and contribution was detected for all peripheral blood lineages. Data are based on two different lentiviral infection/transplant experiments with 3 recipient mice per group (for example, $n = 3$ for Wnt5a^{KD} and Wnt5a-NT mice and $n = 6$ for untransduced mice). **g,** Percentage of B220$^+$, CD3$^+$ and myeloid cells among donor-derived cells in peripheral blood 24 weeks after transplant. *$P < 0.05$; shown are mean values + 1 s.e. Mice were considered as engrafted when the percentage of Ly5.2$^+$ cells in peripheral blood was higher than 1.0 and contribution was detected for all peripheral blood lineages. Data are based on two different lentiviral infection/transplant experiments with 5–7 recipient mice per group (for example, $n = 10$). **h,** Ratio of the densitometric score of the total Cdc42 expression as shown in Fig. 4d. The experiment was repeated four times with mice (1 mouse for 1 sample) from different lentiviral infection/ transplant experiments. Shown are mean + 1 s.e., $n = 4$, *$P < 0.05$. **i, j,** Percentage of donor-derived LT-HSCs polarized for Cdc42 (**i**) and tubulin (**j**) 24 weeks after transplant. Shown are mean values + 1 s.e., $n = 4$, ~200 cells scored per sample in total. *$P < 0.05$. **k,** Representative immunofluorescence *z*-stack pictures of tubulin (green) and β-catenin (red) localization in aged Wnt5a-NT (Ly5.2$^+$GFP$^+$) or aged Wnt5a^{KD} (Ly5.2$^+$GFP$^+$) LT-HSCs. Nuclei are stained with DAPI (blue). Shown is also the final three-dimensional reconstructed merged image. Scale bar, 5 μm.

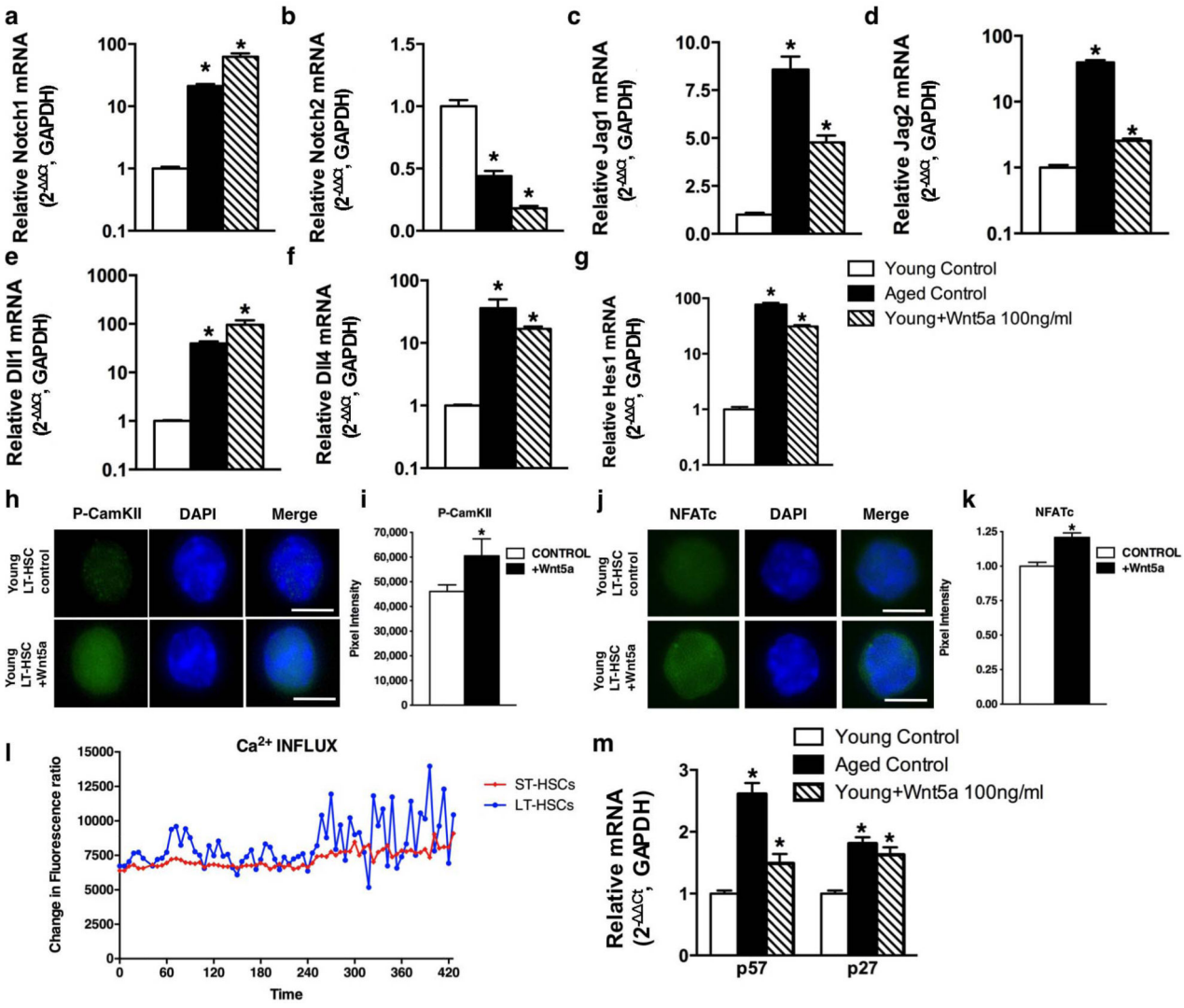

Extended Data Figure 5. Wnt pathways in HSCs and ageing

a–g, Reverse transcriptase real-time PCR analysis of *Notch1*, *Notch2*, *Jag1*, *Jag2*, *Dll1* (delta like1), *Dll4* (delta like 4) and *Hes1* transcript levels in young, aged and young *Wnt5a*-treated (16 h treatment) LT-HSCs. *Notch3*, *Notch4* and *Dll3* (delta like 3) transcripts were below detection limits in all the assayed samples. Data are expressed as fold difference compared to the expression in young LT-HSCs arbitrarily set to 1. Data were analysed with the $2^{-\Delta\Delta Ct}$ method and plotted on a logarithmic or linear scale. Bars are mean + 1 s.e.; $n = 3$, $^{*}P < 0.05$. **h,** Representative immunofluorescence picture of p-CamKII (green) expression and localization in young control and young Wnt5a-treated LT-HSCs. Pictures are shown on a dark background and as overlap with DAPI (staining nuclei). Scale bar, 5 μm. **i,** Relative expression of p-CamKII in young LT-HSCs and on Wnt5a treatment, determined by integration of pixel intensity. $^{*}P < 0.05$. **j,** Representative immunofluorescence picture of NFATc (green) expression and localization in young control and young Wnt5a-treated LT-HSCs. Pictures are shown on a dark background and as overlap with DAPI (staining nuclei). Scale bar, 5 μm. **k,** Relative expression of NAFTc in young LT-HSCs and on Wnt5a

treatment, determined by integration of pixel intensity. *$P < 0.05$. **l,** Changes in intracellular Ca^{2+} concentrations in ST-HSCs and LT-HSCs in response to stimulation with Wnt5a as determined by flow cytometry. **m,** Reverse transcriptase real-time PCR analysis of p57 and p27 transcript levels in young, aged and young Wnt5a-treated (100 ng ml^{-1}, 16 h treatment) LT-HSCs. Data are expressed as fold difference compared to the expression in young LT-HSCs arbitrarily set to 1. Data were analysed with the $2^{-\Delta\Delta Ct}$ method and plotted on a logarithmic or linear scale. Bars are mean + 1 s.e.; $n = 3$, *$P < 0.05$.

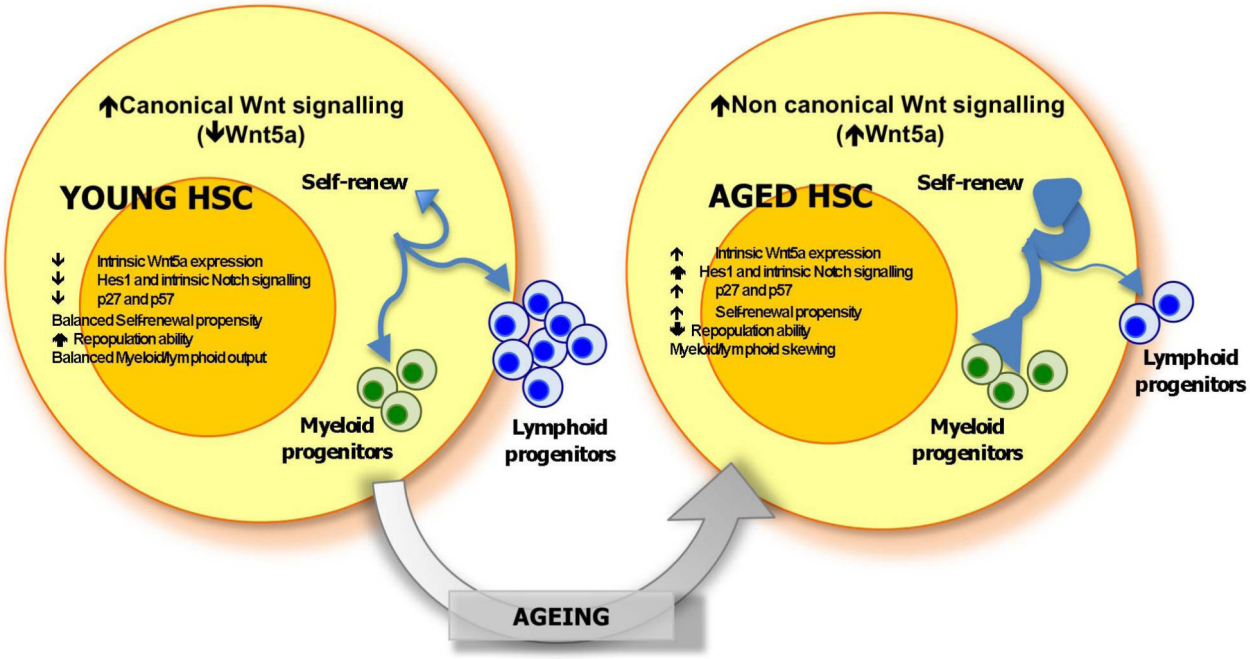

Extended Data Figure 6. Mechanisms of haematopoietic stem-cell ageing

Cartoon scheme summarizing the main phenotypic and functional differences between young and aged LT-HSCs.